Magnetic and Electrical Properties of Nickel Nanoparticles prepared by Hydrazine Reduction Method

Amrut S. Lanje[1*], Satish J. Sharma[2] and Ramchandra B. Pode[3]

[1]Department of Electronics, Dr. Ambedkar College, Chandrapur, India
[2]Department of Electronics, R.T.M. Nagpur University, Nagpur, India
[3]Department of Physics, Kyung Hee University, Seoul, Korea

_____

Abstract

Face centered cubic structure nanocrystalline nickel (Ni) nanoparticles are prepared at 60 °C from $NiCl_2$ precursor using hydrazine hydrate as reducing agent and ethylene glycol as capping agent. Scanning electron microscopy (SEM) shows spherical morphology of Ni nanoparticles with average grain size of 20 nm. Magnetization study reveals ferromagnetic interaction in nickel nanoparticles but close to superparamagnetic state. Saturation magnetization (M_s) at 10 and 300 K are found to be 45 and 40 emu/g respectively. Coercivity (H_c) value at 10 K is found to be 252 Oe. Electrical resistivity of Ni nanoparticles in temperature range   83 – 300 K shows the metallic behavior.

Keywords*: nickel, nanoparticles, ethylene glycol, magnetization, resistivity.*

_____

Introduction

Metal nanoparticles have attracted much attention in the fields of physics, chemistry, electronics and biology [1, 2] because of their unique electrical [3], chemical [4], optical [5] and photo-electrochemical [6] properties, which are strongly dependent on the sizes and shapes of metal nanomaterials [7–9]. Metal nanoparticles have a high specific surface area and a high surface to volume ratio. Nanostructured noble metals are potentially used in catalysis, optoelectronics, microelectronics etc. The ultrafine and nanometer nickel powders have attracted a great deal of attention over past decades due to their specific properties such as magnetism, thermal resistance, chemical activity and have a wide range of applications including batteries, hard alloy, catalyst, electricity and so on [10]. It is reported that nickel powder has been produced for multilayer ceramic capacitors in cellular phones and mobile computers [11].

Many techniques have been used to prepare the metal nanoparticles, such as chemical reduction [11-18], electrochemical reduction [19, 20], photochemical reduction [21, 22],

sonochemical method [23], microemulsion technique [24], polyol process [25, 26], alcohol reduction [27], heat evaporation [28, 29] and many others [30, 31]. The physical methods always need a high temperature (over 1000 ºC) [29], vacuum and expensive equipments, but the conditions that the chemical methods needed are not so critical. The chemical reduction method is one of the commonest method to synthesize colloidal metal particles because of its convenient operation, easy controlling and simple equipments needed.

Metal nanoparticles of nickel, iron and cobalt are relatively difficult to synthesis because they easily get oxidized. Among them, nickel is the most stable particle. Nickel nanoparticles have important applications in catalysis and magnetic materials [30]. However, few literatures on the preparation of metal nanoparticles have been reported. In present work, we have prepared nickel nanoparticles using hydrazine reduction method and magnetic and electrical properties of prepared sample are studied.

In the absence of soluble polymer or other extra protective agent, synthesis of nickel nanoparticles in ethylene glycol with hydrazine hydrate as protective agent as well as reducing agent is performed.

Materials and Methods

Nickel chloride hexahydrate ($NiCl_2 . 6H_2O$, 98 % pure) and hydrazine hydrate (99 %) were obtained from Kemphasol, Mumbai. Sodium hydroxide (NaOH) pellets extra pure was obtained from Loba Chemie. Ethylene glycol was supplied by Merck, India. The deionized water was used through out the experiment. Ni sample is prepared using Nickel chloride hexahydrate ($NiCl_2 . 6H_2O$) as a precursor and hydrazine hydrate as reducing agent following the methods reported earlier [32-34].
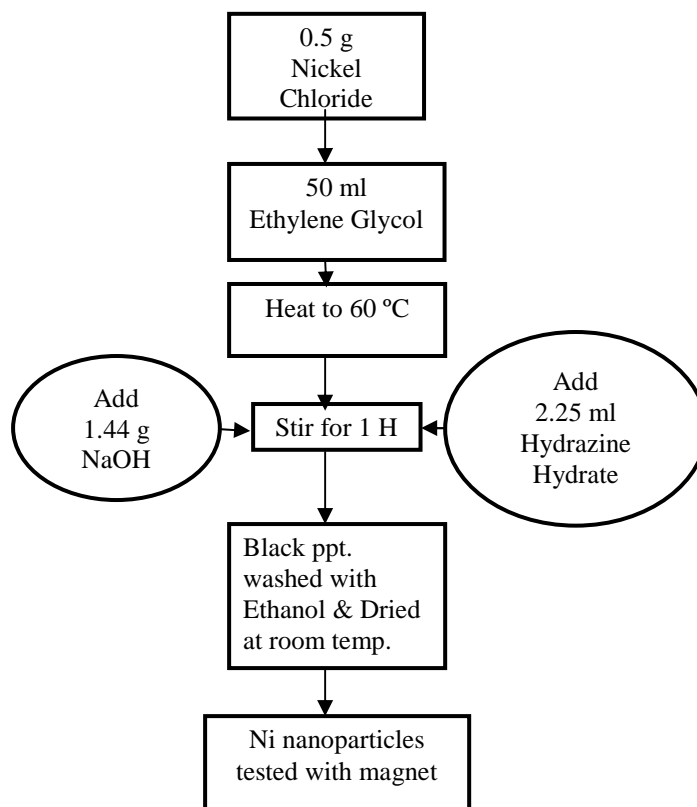
0.5 g of nickel chloride is dissolved in 50 ml ethylene glycol. The solution is heated to 60 ºC. Then 2.25 ml hydrazine hydrate is added to above solution. 1.44 g of NaOH (1M) solution is added with stirring. The complete solution is kept under magnetic stirrer for 1 h at 60 ºC. After 1 h reaction is completed and black nickel nanoparticles are formed. These nanoparticles are collected, washed several times by ethanol and dried in the room temperature. Figure 1 shows flowchart for the preparation of nickel nanoparticles.

The reduction reaction can be expressed as

$$2Ni^{2+} + H_4N_2 + 4OH^- \rightarrow 2Ni + N_2 + 4H_2O$$
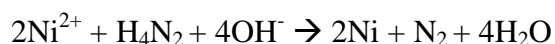
It is seen that N_2 gas is continuously bubbled up in the reaction. It automatically creates N_2 atmosphere during the reaction. Hence, no extra N_2 gas is required for the synthesis of nickel nanoparticles.

The powder X-ray diffraction (XRD) is performed using Philips Holland, XRD system PW 1710 with nickel filtered CuK_α (λ = 1.5405 Å) radiation. The average crystallite size (*t*) has been calculated from the line broadening using the Scherrer's relation: $t = K\lambda / \beta cos\theta$, where *K* is a constant (~1), β is full width at half maximum (FWHM) and θ is Bragg's angle. The scanning electron microscopy (SEM) is performed with JEOL JSM-5600. Magnetization of nickel nanoparticles are carried out using PPMS VSM of Quantum Design. The resistivity is measured using fully automated four-probe method.

```
                    ┌─────────────┐
                    │   0.5 g     │
                    │   Nickel    │
                    │  Chloride   │
                    └─────────────┘
                          │
                          ▼
                    ┌─────────────┐
                    │    50 ml    │
                    │Ethylene Glycol│
                    └─────────────┘
                          │
                          ▼
                    ┌─────────────┐
                    │ Heat to 60 ℃ │
                    └─────────────┘
                          │
        ╭─────────╮       ▼        ╭──────────╮
        │  Add    │  ┌──────────┐  │   Add    │
        │ 1.44 g  │─▶│Stir for 1 H│◀─│ 2.25 ml  │
        │  NaOH   │  └──────────┘  │ Hydrazine│
        ╰─────────╯       │        │ Hydrate  │
                          ▼        ╰──────────╯
                    ┌─────────────┐
                    │ Black ppt.  │
                    │ washed with │
                    │Ethanol & Dried│
                    │at room temp.│
                    └─────────────┘
                          │
                          ▼
                    ┌─────────────┐
                    │Ni nanoparticles│
                    │tested with magnet│
                    └─────────────┘
```

Figure 1. Flowchart for the preparation of nickel nanoparticles

Results and Discussion

**Structural and particle size studies**

Figure 2 (a) shows X-ray diffraction pattern of prepared nickel nanoparticles. The intensity is determined in the range $20° < 2\theta < 90°$ with 0.02 degree step size. The 2θ values for the planes (111), (200) and (220) are found to be 44.5°, 51.94° and 76.42° respectively. The XRD pattern shows cubic structure of sample and having a single-phase. No distinct diffraction peak other than those from fcc-Ni is found in the sample. The lattice constant is $a = 3.4392$ Å and unit cell volume is $V = 40.6757$ Å^3, matched with JCPDS file no. 04-850 as shown in figure 2 (b). The broad diffraction peaks are due to nano-size of particles. Maximum intensity peak (111) was used to estimate the crystallite size and it is found to be 18 nm using Scherrer equation.

Figure 3 shows SEM image of nickel nanoparticles. The shape of the Ni particles is spherical and are linked together to form chains. The average grain particle size is about 20 nm which closed to the crystallite size calculated from XRD. The formation of particle aggregates or magnetic clusters are observed due to strong interaction among the magnetic dipoles of nickel nanoparticles.
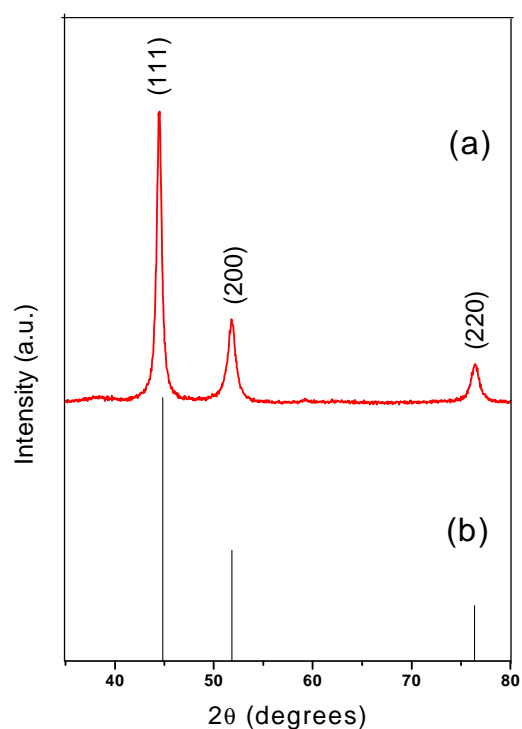
**Figure 2. (a) XRD pattern of prepared nickel nanoparticles
(b) JCPDS file no. 04-850**
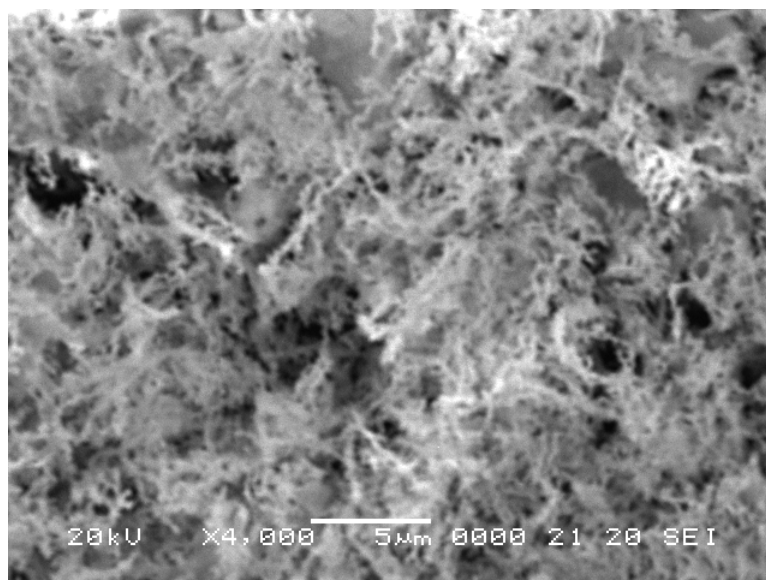
Figure 3. SEM image of nickel nanoparticles

Magnetic Study

Figure 4 shows the variation of magnetization with magnetic field (M-H loop) at 10 and 300 K. Saturation magnetization (M_s) and coercivity (H_c) decreases at 300 K for nickel nanoparticles compared to bulk nickel (Table I). At 300 K, M_s and H_c are found to be 40.5 emu/g and 86.5 Oe, respectively. The value of M_s in bulk nickel is 54.4 emu/g [35].

52

Reduction in magnetization is related to particle size effect. Decrease in M_s is due to decrease in particle size which may also results to increase in surface area. Due to small particle size surface to volume ratio increases and hence M_s reduces at 300 K. Decrease in M_s can also be attributed to superparamagnetic behavior in nickel nanoparticles. Remanence magnetization (M_r) is slightly greater than the bulk nickel may be due to presence of microstructures in the sample.

M_s, M_r and H_c values are increased in nickel nanoparticles at 10 K (see Table I). When particle gets freeze, thermal energy of nickel particles gets decreases which results in increase of H_c. At lower temperature some atiferromagnetic nickel oxides layers are formed above the ferromagnetic nickel nanoparticles. The value of M_s increases due to pinning of these antiferromagnetic nickel oxides on ferromagnetic nickel nanoparticles. The magnetization increases rapidly with a small magnetic field and it attains a maximum value when magnetic field of 50 KOe is applied.
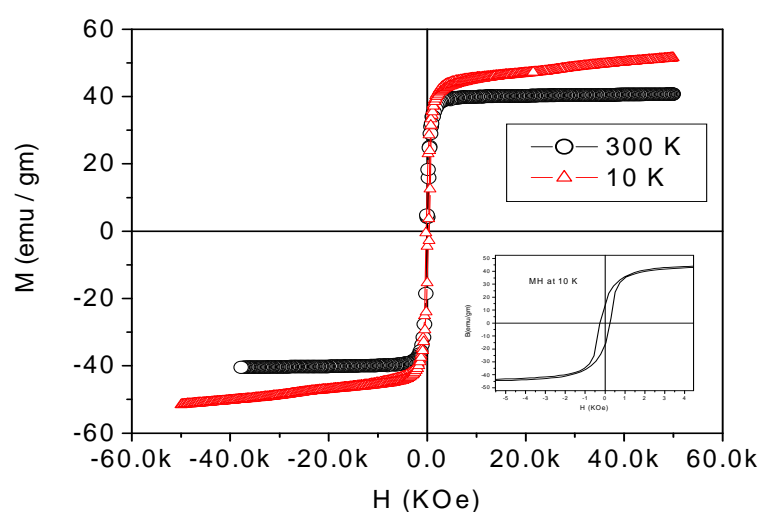

Figure 4. Variation of magnetization (M) with magnetic field (H) at 10 and 300 K for 20nm nickel nanoparticles. Inset of figure shows enlargement of low field data at 10 K

Table I. Comparative values of M_s, M_r and H_c in bulk and nickel nanoparticles

Nickel	Temperature	M_s (emu /g)	M_r (emu /g)	H_c (Oe)
Bulk	300 K	54.4	2.7	100
Nano (20 nm)	300 K	40.5	6.9	86.5
Nano (20 nm)	10 K	50.3	13.5	252

Figure 5 shows variation of magnetization with temperature at magnetic field of 0.05 T.
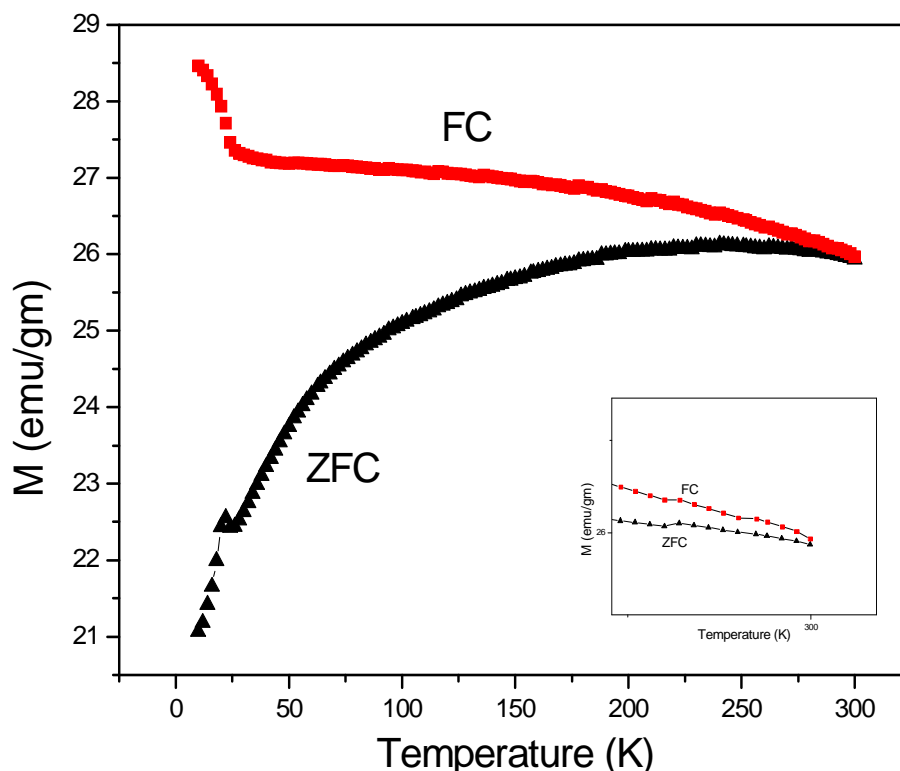
Figure 5. Temperature dependence ZFC and FC magnetization for nickel nanoparticles Inset of figure shows enlargement of FC and ZFC curve at 300 K

The sample of nickel nanoparticles is first cooled at zero fields down to lowest temperature, then a field of 0.05 tesla is applied to get zero field cooled (ZFC) magnetization. The sample is then cooled down keeping magnetic field constant to get field cooled (FC) magnetization. Both ZFC and FC magnetization are recorded at 0.05 T. ZFC curve is different from FC curve. There is a narrow cusp at 22 K in ZFC curve due to decrease in thermal energy. The magnetization increases with temperature below 300 K. It is also observed that FC and ZFC curves do no meet together (Inset fig. 5). It reveals ferromagnetic interaction in nickel nanoparticles but close to superparamagnetic state.

3.3 Electrical resistivity measurement
For measurement of electrical resistivity of nickel nanoparticles fully automated four-probe resisitivity measurement set-up is used. The pellet of nickel nanoparticles is prepared using hydraulic press and 10 mm size die and punch.

Prepared pellet is cut in rectangular size having thickness (t) = 0.0545 cm, width (b) = 0.169 cm and length (L) = 0.19 cm (distance between voltage probes). Cross sectional area (A) = 0.00921 cm^2. The resistivity (ρ) is calculated using the formula:

$$\rho = \left(\frac{A}{L}\right) * R.$$
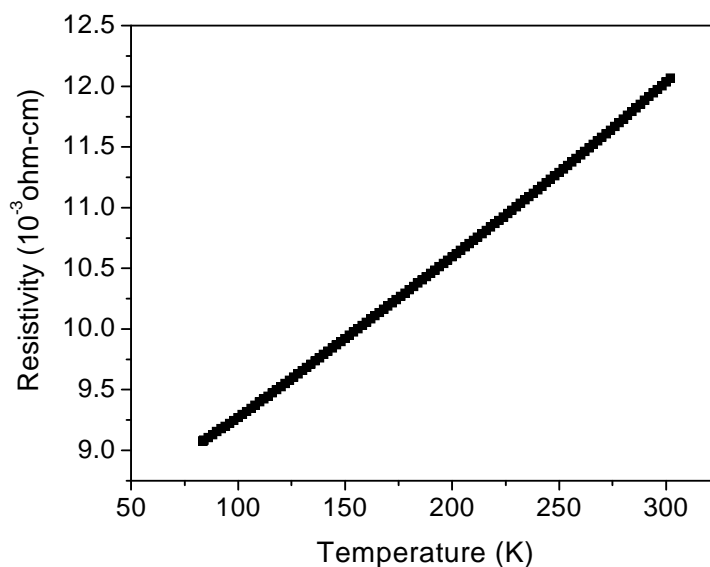
Figure 6. Variation of resistivity with temperature for nickel nanoparticles

Figure 6 shows variation of resistivity with respect to temperature. Electrical resistivity of nickel nanoparticles in low temperature range 83 – 300 K is measured. It is found that the resistivity is 9 x 10^{-3} Ω-cm at 83 K and 12 x 10^{-3} Ω-cm at 300 K. The resistivity of nickel nanoparticles is high as compare to bulk nickel due decrease in thermal energy. It increases with temperature indicating metallic nature.

Conclusion

Face centered cubic (fcc) structure nickel nanoparticles are prepared using simple and low cost precipitating method. Magnetization study reveals ferromagnetic interaction in nickel nanoparticles but close to superparamagnetic state at 300 K. Saturation magnetization value is less than that of bulk indicating particle size effect. At low temperature (83 – 300 K) the electrical resistivity is increases with temperature. It is found that resistivity of nickel nanoparticles is high as compare to bulk nickel due to decrease in thermal energy.

Acknowledgments

References

[1] G Schmid. Clusters and Colloids: from Theory to Applications, VCH, Weinheim, **1994**.
[2] A Henglein. *Chem. Rev*., **1989,** 89, 1861.
[3] G Peto; GL Molnar; Z Paszti; O Geszti; A Beck; L Guczi. *Mater. Sci*. Eng**., 2002**, C 19, 95.

[4] A Kumar; S Mandal; PR Selvakannan; R Pasricha; AB Mandale; M Sastry. *Langmuir*, **2003**, 19, 277.

[5] A Krolikowska; A Kudelski; A Michota; J Bukowska. *Surf. Sci.,* **2003**, 532, 227.

[6] N Chandrasekharan; PV Kamat. *J. Phys. Chem.,* **2000,** B 104**,** 10851.

[7] JA Creighton; DG Eadon. *J. Chem. Soc., Faraday Trans.,* **1991**, 24, 3881.

[8] ZB Zhang; XZ Sun; MS Dresselhaus; JY Ying. *Phys. Rev.,* **2000**, B 61, 4850.

[9] K Liu; K Nagodawithana; PC Searson; CL Chien. *Phys. Rev.,* **1995**, B 51**,** 7381.

[10] Z Ying; J Shengming; Q Guanzhou; Y Min. *Mater. Sci. Eng.,* **2005**, B 122, 222.

[11] KS Chou; CY Ren. *Mate. Chem. Phys.,* **2000**, 64, 241.

[12] P Christophe; L Patricia; P Marie-Paule. *J. Phys. Chem.* **1993,** 97, 12974.

[13] SA Vorobyova; AI Lesnikovich; NS Sobal. *Colloid. Surf.,* **1999**, A 152, 375.

[14] Z Zhang; B Zhao; L Hu. *J. Solid State Chem.*, **1996**, 121, 105.

[15] IM Yakutik; GP Shevchenko. *Surf. Sci.,* **2004,** 414, 566.

[16] H Huang; X Yang. *Carbohyd. Res.,* **2004,** 339, 2627.

[17] Z Zhang; M Han. *Chem. Phys. Lett.,* **2003,** 374, 91.

[18] Y Tan; Y Wang; L Jiang. *J. Colloid Interface Sci.,* **2002,** 249, 336.

[19] Y C Liu; LH Lin. *Electrochem. Commun.* **2004,** 6, 1163.

[20] H Sandmann; Dietz; W Plieth. *J. Electroanal. Chem.,* **2000,** 491, 78.

[21] K Mallick; MJ Witcomb; Scurrell. *Mater. Chem. Phys.,* **2005,** 90, 221.

[22] S Keki; J Torok; G Deak. *Colloid Interface Sci.,* **2000,** 229, 550.

[23] Y Mizukoshi; K Okitsu; Y Maeda; TA Yamamoto; R Oshima; Y Nagata. *J. Phys. Chem.,* **1997,** B 101, 7033.

[24] K Osseo-Asare; FJ Arriagada. *Ceram. Trans.,* **1990,** 12, 3.

[25] LK Kurihara; GM Chow; PE Schoen. *Nanostruct. Mater.,* **1995,** 5, 607.

[26] RS Ningthoujam; NS Gajbhiye; S Sharma. *Pramana,* **2009**, 72, 577.

[27] HH Huang; XP Ni; GL Loy; CH Chew; KL Tan; FC Loh; JF Deng; GQ Xu. *Langmuir*, **1996,** 12, 909.

[28] CH Bae; SH Nam; SM Park. *Appl. Surf. Sci.,* **2002,** 628, 197.

[29] AB Smetana; KJ Klabunde; *J. Colloid Interface Sci.,* **2005,** 284, 521.

[30] SH Wu; DH Chen. *J. Colloid Interface Sci.,* **2003,** 259, 282.

[31] Něel l. Ann. *Geophys.,* **1949**, 5, 99.

[32] Szu-Han Wu; Dong-Hwang Chen. *J. Colloid Interface Sci.,* **2003,** 259, 282.

[33] P Saravanan; TA Jose; PJ Thomas; GU Kulkarni. *Bull. Mater. Sci.,* **2001,** 24, 515.

[34] F Fievet; JP Lagier; M Figlarz. *Sol. State Ionics,* **1995,** 82, 53.

[35] BD Cullity. Introduction to Magnetic Materials, Addison-Wesley, USA, **1972**.